

Electromagnetic radiations and polarized images of synchrotron radiations in curved spacetime

Zezhou Hu¹, Yehui Hou¹, Haopeng Yan², Minyong Guo^{3*} Bin Chen^{1,2,4}

¹*Department of Physics, Peking University, No.5 Yiheyuan Rd, Beijing 100871, P.R. China*

²*Center for High Energy Physics, Peking University, No.5 Yiheyuan Rd, Beijing 100871, P. R. China*

³*Department of Physics, Beijing Normal University, Beijing 100875, P. R. China*

⁴*Collaborative Innovation Center of Quantum Matter, No.5 Yiheyuan Rd, Beijing 100871, P. R. China*

Abstract

Electromagnetic radiation of charged particles in a curved spacetime has not been studied thoroughly in a covariant way. In this work we derive a universal covariant formula of the electric field vector of electromagnetic radiation in any curved spacetime employing the method proposed by DeWitt and Brehme in [1]. Our work shows the Einstein's equivalence principle holds for electromagnetic radiation under the geometric optics approximation. In particular, we find compact covariant formulas encoding the intensity and polarization direction of synchrotron radiations. We also construct a toy model to calculate the polarized images of synchrotron radiations in Schwarzschild black hole spacetime and discuss the applications in understanding the polarized image of black hole photon ring observed by the Event Horizon Telescope.

* Corresponding author: minyongguo@bnu.edu.cn

1 Introduction

In 2019, the Event Horizon Telescope (EHT) Collaborations published the first images of a supermassive black hole in M87 [2]. This opened a new window to study various problems in strong-field gravity and the physics in accretion disk via electromagnetic signatures. Very recently the EHT Collaborations released the polarized images of the black hole [3, 4], which reveal a bright ring of emission with a twisting polarization pattern and a prominently rotationally symmetric mode. The polarized images originate from the polarized synchrotron radiations from electrons orbiting the black hole. Over the past few decades, people have been trying to simulate the polarimetric images of black holes in order to understand the properties of accretion disk and spacetime geometry [5–15]. For the recent study on the polarized images of black hole, see [16–22]

In fact, the problem of electromagnetic radiations of charged particles in curved spacetime has not been completely solved from the perspective of general relativity. In the literatures, the currently used model of synchrotron radiation (as a type of electromagnetic radiation) in a curved spacetime, is based on the electrodynamics in the instantaneous inertial frame of the charged particles. This treatment relies on the Einstein’s Equivalence Principle (EEP) and the belief that one could just borrow the results from the classical electrodynamics in a flat spacetime to study phenomena in astrophysics. It works fine in most of realistic situations that the physics of interest is far from a strong gravitational system and the spacetime curvature is ignorable.

However, the above approach is not satisfactory, both from theoretical and practical points of view. Although we are allowed to use the results of flat spacetime to deal with the electromagnetic radiation problem when the gravity is not strong enough, it is essential to find the covariant formula of electromagnetic radiation of charged particles in curved spacetime, which not only allow us to read the general relativistic effects on the radiation but also is indispensable in studying the radiation in the strong field region. This is similar to the situation that even the particle move locally in a uniform motion, it actually takes geodesic motion in a coordinate chart. In practice, the transformation from the radiation in local flat spacetime to the one in a curved spacetime is not always convenient and sufficient, especially when we want to study not only the local properties of the radiations. Furthermore, as a matter of fact, the EEP has been found to be not generally true for the charged particles moving in curved spacetime [1]. Hence, a natural question to us is under what condition the EEP works well for a charged radiating particle in curved spacetime?

In this work, we address the issues mentioned above in electromagnetic radiation in curved

spacetime. Our discussions will be based on the pioneering work by DeWitt and Brehme (DB) in [1], in which the authors paid their main attention to radiation damping to understand the EEP. Here we pushed their work in a slightly different direction and discuss the electromagnetic radiations and synchrotron radiations. We derive a universal covariant formula of electromagnetic radiations of charged particles in curved spacetime which includes a tail term from the curvature of spacetime and find the EEP stands in the geometric optics approximation, that is, the frequencies of radiated photons are large enough. In particular, by considering charged particles that accelerated only by magnetic fields, we obtain compact covariant formulas encoding the intensity and polarization direction of synchrotron radiations which would help us to understand the nature of the polarized EHT image.

The remaining part of this paper is organized as follows. In Sec. 2, we set up our problems of interest and find the expression of the polarization vector. In Sec. 3, we complete other theoretical preparations for calculating the polarized image of synchrotron radiations around a Schwarzschild black hole, In Sec. 4, we show some specific examples. In Sec. 5, we summarize and conclude this work.

2 Set up

We set up our research problems and models in this section. We focus our attention on a black hole immersed in uniform magnetic fields. Since we would like to consider polarizations of synchrotron radiations emitted from the relativistic charged particles moving near the black hole, first of all, we need to know the polarization vector of synchrotron radiations which take the form of electromagnetic waves. That is to say, our task is to find the electromagnetic radiation produced by a moving source orbiting near a black hole.

2.1 Bi-tensors and Green's functions in curved spacetime

In flat spacetime, the radiation of a moving charged particle has been well-studied[23]. By using the retarded Green's function, the gauge potential caused by a charged particle in motion is simply

$$A_\mu(x) = 4\pi \int d^4x' G_{\mu\alpha}^{\text{ret}}(x - x') J^\alpha(x'), \quad (2.1)$$

where the current is induced by the moving charged particle

$$J^\alpha(x') = e \int d\tau Z^\alpha(\tau) \delta^{(4)}(x' - z_0(\tau)). \quad (2.2)$$

Z^α is the 4-velocity of the particle and $z_0(\tau)$ characterize the worldline of the particle. The corresponding gauge potential is known as the *Liénard-Wiechert* potential. The corresponding

field strength consists of two parts: one part being independent of the acceleration is the static field; while the other part, depending linearly on the acceleration, is the radiation field.

In curved spacetime, the similar radiation problem has been addressed by DB in [1] in order to understand the radiation damping and the Equivalence Principle for the charged particle in motion. Next, we would like to give a brief and necessary review of the pioneering work by DB. A key point in DB's treatment is to develop the theory of bi-tensors connecting the tensor fields at two different spacetime points x and z , in order to study the covariant Green's functions. (For a different approach using the vielbein formalism, see [24]).

We closely follow DW's conventions. Let z be the point of the source and x be other points in the spacetime. The letters of Greek alphabet α to κ in are assigned to the point z , while indices taken from λ to ω are left to the points x . For example, z^α and x^μ are the coordinates of z and x , respectively. $s(x, z)$ is defined as the bi-scalar of geodesic interval, which denotes the length of the geodesic connecting x and z . Obviously, we can conclude that $\lim_{z \rightarrow x} s(x, z) = 0$, and furthermore we can see that $s(x, z) = ds(x)$ when considering $z = x + dx$, that is to say, at this moment we can take s as the proper time of the geodesic through the point x . Moreover, $s > 0$ denotes a spacelike interval and $s < 0$ means the interval is timelike, while $s = 0$ defines the light cone. Given a sufficient large interval, s may change sign. However, if we focus on a small neighborhood of a given source, the geodesic interval is single-valued, and thus the covariant expansions can be performed to identify the asymptotic forms of Green's functions containing the information of the electromagnetic waves. It turns out to be convenient to introduce the quantity

$$\sigma \equiv \pm 1/2s^2, \quad (2.3)$$

to avoid the "branch point" problem, which is positive for space-like intervals and negative for time-like ones.

Furthermore, in addition to the ordinary tensors which act on the point z or x , we need to introduce bi-tensors, of which some indices refer to the point z and the other ones refer to the point x . For example, we have a bi-vector $T_{\mu\alpha}$, in which μ refers to the point x and α refers to the point z . Then, it is useful to introduce the bi-vector of geodesic parallel displacement, denoted by $\bar{g}_{\mu\alpha}(x, z)$, which plays the role of transforming the given bi-tensor into a new bi-tensor all of whose indices refer to the same point. The definition of $\bar{g}_{\mu\alpha}$ is given by the following equations

$$\nabla^\nu \sigma \nabla_\nu \bar{g}_{\mu\alpha} = 0, \quad \nabla^\gamma \sigma \nabla_\gamma \bar{g}_{\mu\alpha} = 0, \quad \lim_{x \rightarrow z} \bar{g}_\mu^\alpha = \delta_\mu^\alpha.$$

For a local vector V_μ at the point x , it can be generated from V_α at the point z by parallel

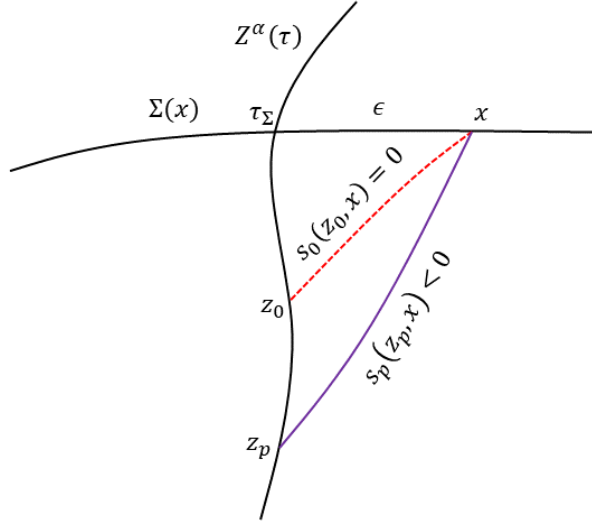


Figure 1: A diagram of radiations at the field point x on a spacelike hypersurface $\Sigma(x)$. Z^α is the 4-velocity of the charged source.

displacement along the geodesic from z to x , that is, $V_\mu = \bar{g}_\mu^\alpha V_\alpha$. Similarly, one can easily apply the geodesic parallel displacement to local tensors of arbitrary order. For the purpose of our work, we are not going to show more details of bi-tensors, which can be found in [1].

Since we are interested in the electromagnetic radiation, we next turn to the solutions of the covariant vector wave equations, which take the form

$$\nabla^\nu \nabla_\nu A_\mu + R_\mu^\nu A_\nu = J_\mu, \quad (2.4)$$

in the Lorenz gauge $\nabla_\mu A^\mu = 0$. The retarded Green's function for the vector wave equation can be formally expressed as

$$G_{\mu\alpha}^{\text{ret}}(x, z) = 2\Theta[\Sigma(x), z]\bar{G}_{\mu\alpha}(x, z), \quad (2.5)$$

where z is the source point, $\Sigma(x)$ is an arbitrary spacelike hypersurface containing the field point x , and $\Theta[\Sigma(x), z] = 1 - \Theta[z, \Sigma(x)] = 1$ when z lies to the past of $\Sigma(x)$ and $\Theta[\Sigma(x), z] = 0$ when z lies to the future. The ‘‘symmetric’’ Green's function $\bar{G}_{\mu\alpha}(x, z)$ reads[?]]

$$\bar{G}_{\mu\alpha}(x, z) = (8\pi)^{-1}[u_{\mu\alpha}\delta(\sigma) - v_{\mu\alpha}\theta(-\sigma)] \quad (2.6)$$

where $\delta(\sigma)$ is the δ -function and θ is the Heaviside function. $u_{\mu\alpha} \propto \bar{g}_{\mu\alpha}$ and $v_{\mu\alpha}$ are bi-vectors, both of which are determined by solving the vector wave equation (2.4). The term $u_{\mu\alpha}\delta(\sigma)$ shows that a sharp pulse of electromagnetic radiation travels along the null geodesics between the source z and the field x , with its polarization vector being parallel-transported. The other term $v_{\mu\alpha}\theta(-\sigma)$ in the Green's function, often referred to as the ‘‘tail’’ term, describe

the electromagnetic radiations produced by the source whose geodesic intervals $s(z, x)$ are timelike. It shows that the sharp pulse can develop a “tail”, due to the scattering with the “bump” in a curved spacetime. In Fig. 1, we show the radiations received at a field point x on $\Sigma(x)$.

2.2 Electromagnetic fields near a point particle

The Green’s functions $\bar{G}_{\mu\alpha}(x, z)$ cannot be solved exactly in a generic curved spacetimes. Nevertheless, we can do covariant expansions of $\bar{G}_{\mu\alpha}(x, z)$ around z to obtain the electromagnetic fields generated from the source in the very near region of point z . In particular, since we are interested in the synchrotron radiations emitted from non-geodesic charged particles, we only need to include the contributions from the history of the particle at and before the point z_0 in order to determine the electromagnetic field at point x in Fig. 1. As shown in Fig. 1, Z^α is the tangent vector of the world line of the source, and the proper time is set to be τ . For any τ , one always has a certain spacelike hypersurface Σ whose normal vector is Z^α . Then the induced metric on Σ can be defined as $h^{\alpha\beta} = g^{\alpha\beta} + Z^\alpha Z^\beta$. Let us say at the proper time τ_Σ , the source arrives at the point z . We introduce a fixed field point x which has a small spatial distance ϵ deviated from z_Σ on the hypersurface Σ , and in terms of the induced metric, we can have the following relation:

$$\epsilon^2 = h^{\alpha\beta} \nabla_\alpha \sigma \nabla_\beta \sigma + (\text{higher orders in } \epsilon). \quad (2.7)$$

This relation tells us that the quantities like $\nabla_\mu \sigma$ is of order $\mathcal{O}(\epsilon)$. For each geodesic interval s connecting the source point z and the field point x , following the results in [1], we can have the expansions of the bi-vectors:

$$\begin{aligned} u_{\mu\alpha} &= \left[1 - \frac{1}{12} R^{\beta\gamma} \nabla_\beta \sigma \nabla_\gamma \sigma + \mathcal{O}(\epsilon^3) \right] \bar{g}_{\mu\alpha}, \\ v_{\mu\alpha} &= -\frac{1}{2} \bar{g}^\beta_\mu \left(R_{\alpha\beta} - \frac{1}{6} g_{\alpha\beta} R \right) + \mathcal{O}(\epsilon), \end{aligned} \quad (2.8)$$

and

$$\begin{aligned} \nabla_\beta \sigma \nabla_\alpha \sigma &= g_{\alpha\beta} + \frac{1}{3} R_{\alpha\beta}^{\gamma\delta} \nabla_\gamma \sigma \nabla_\delta \sigma + \mathcal{O}(\epsilon^3), \\ \nabla_\beta \bar{g}_{\mu\alpha} &= -\frac{1}{2} R_{\delta\alpha\beta}^{\gamma} \nabla_\gamma \sigma + \mathcal{O}(\epsilon^2), \\ \nabla_\beta u_{\mu\alpha} &= \left(-\frac{1}{2} \bar{g}^\delta_\mu R_{\delta\alpha\beta}^{\gamma} - \frac{1}{6} \bar{g}_{\mu\alpha} R^\gamma_\beta \right) \nabla_\gamma \sigma + \mathcal{O}(\epsilon^2). \end{aligned}$$

Here we want to emphasize that the so-called higher order terms $\mathcal{O}(\epsilon^2)$ and $\mathcal{O}(\epsilon^3)$ mean the corresponding terms involve two and three covariant derivatives of σ respectively. Thus, the

above expansions are valid for any kind of geodesic interval s , even for the geodesic intervals on the light cone with $s = 0$.

With the expansions of the Green's functions, the retarded gauge potential of a point charged particle reads

$$\begin{aligned} A_\mu^{\text{ret}} &= 4\pi e \int_{-\infty}^{+\infty} G_{\mu\alpha}^{\text{ret}} Z^\alpha d\tau \\ &= -e \left[u_{\mu\alpha} Z^\alpha (\nabla_\beta Z^\beta)^{-1} \right]_{\tau=\tau_0} + e \int_{-\infty}^{\tau_0} v_{\mu\alpha} Z^\alpha d\tau \end{aligned}$$

where we have defined τ_0 as the proper time of the point particle at the point z_0 in Fig. 1, and e is the charge of the particle. The corresponding electromagnetic field strength tensor can be obtained by straightforward differentiation

$$\begin{aligned} F_{\mu\nu}^{\text{ret}} &= 2e [Z^\alpha \nabla_{[\mu} \sigma u_{\nu]\alpha} (Z^\beta Z^\gamma \nabla_\beta \nabla_\gamma \sigma) (D_\tau \sigma)^{-3} \\ &\quad - (Z^\alpha D_\tau \nabla_{[\mu} \sigma u_{\nu]\alpha} + D_\tau Z^\alpha \nabla_{[\mu} \sigma u_{\nu]\alpha}) (D_\tau \sigma)^{-2} \\ &\quad + Z^\alpha (\nabla_{[\mu} u_{\nu]\alpha} + \nabla_{[\mu} \sigma v_{\nu]\alpha}) (D_\tau \sigma)^{-1}]_{\tau=\tau_0} \\ &\quad - 2e \int_{-\infty}^{\tau_0} d\tau Z^\alpha \nabla_{[\mu} v_{\nu]\alpha} \end{aligned} \quad (2.9)$$

where we have introduced the derivative operator along the vector Z^α , that is, $D_\tau \equiv Z^\beta \nabla_\beta$. In Eq. (2.9), the leading terms of $F_{\mu\nu}^{\text{ret}}$ are of order $\mathcal{O}(\epsilon^{-2})$, and they are in fact from the Coulomb potential which would give a renormalization of the mass of the point particle but won't contribute to the radiations. The subleading terms being of order $\mathcal{O}(\epsilon^{-1})$ from the lightlike part would contribute to the radiations mostly. The synchrotron radiations originating from the gravity involving curvature tensors are of order $\mathcal{O}(\epsilon^0)$ both in the lightlike part and in the "tail" part. The radiations from the complicated "tail" term involve the integrations over the whole past history of the particle, and they won't be observed if we only observe for a narrow time-interval. Moreover, such radiations are sub-leading, but could be important in a strong gravitational field.

2.3 Synchrotron radiations and polarization vector

Next, we turn to find out the electromagnetic radiations and synchrotron radiations generated by a non-geodesic point particle acted upon by the Lorentz force, and extract the corresponding electric component as the polarization vector, as well as its intensity.

Note that the geodesic interval between the point z_0 and the point x is on the light cone, thus, we are allowed to define $\nabla_\alpha \sigma \equiv \epsilon k_\alpha$ at the point z_0 , where $k_\alpha k^\alpha = 0$ is a null vector along the light cone. Then, it's easy to conclude that at the point x , we have $\nabla_\mu \sigma = -\bar{g}_\mu^\alpha \nabla_\alpha \sigma =$

$-\epsilon k_\mu$. After some calculations, the electromagnetic field tensor in Eq. (2.9) can be expanded and rewritten as

$$F_{\mu\nu}^{\text{ret}} = \sum_{d=-2}^{\infty} F_{\mu\nu}^{(d)} \epsilon^d + (\text{tail part}), \quad (2.10)$$

where

$$F_{\mu\nu}^{(-2)} = 2e \left[Z^\alpha k_{[\nu} \bar{g}_{\mu]\alpha} (k_\eta Z^\eta)^{-3} \right]_{\tau=\tau_0} \quad (2.11)$$

$$F_{\mu\nu}^{(-1)} = 4e \left[k_{[\nu} \bar{g}_{\mu]\alpha} (k_\beta D_\tau Z^{[\beta} Z^{\alpha]}) (k_\eta Z^\eta)^{-3} \right]_{\tau=\tau_0} \quad (2.12)$$

$$\begin{aligned} F_{\mu\nu}^{(0)} = 2e & \left\{ k_{[\nu} \bar{g}_{\mu]\alpha} Z^\alpha \left(\frac{1}{3} R_{\gamma\beta}{}^\theta{}^\delta k_\theta k_\delta Z^\beta Z^\gamma + \frac{1}{12} R^{\beta\gamma} k_\beta k_\gamma \right) (k_\eta Z^\eta)^{-3} \right. \\ & + \left(\frac{1}{2} k_{[\nu} \bar{g}_{\mu]}{}^\delta R_{\delta\alpha\beta}{}^\gamma + \frac{1}{6} k_{[\nu} \bar{g}_{\mu]\alpha} R_\beta{}^\gamma \right) k_\gamma Z^\alpha Z^\beta (k_\eta Z^\eta)^{-2} \\ & + \frac{1}{6} \bar{g}_{[\nu}^\theta{}_{\mu]\alpha} R_{\theta\beta}{}^\delta{}^\gamma k_\gamma k_\delta Z^\alpha Z^\beta (k_\eta Z^\eta)^{-2} \\ & - Z^\alpha \left[k_\gamma \left(\frac{1}{2} \bar{g}_{[\nu}^\beta{}_{\mu]}{}^\delta R_{\delta\alpha\beta}{}^\gamma + \frac{1}{6} \bar{g}_{[\nu}^\beta{}_{\mu]\alpha} R_\beta{}^\gamma \right) \right. \\ & \left. \left. + \frac{1}{2} k_{[\nu} \bar{g}_{\mu]}{}^\beta \left(R_{\alpha\beta} - \frac{1}{6} g_{\alpha\beta} R \right) \right] (k_\eta Z^\eta)^{-1} \right\}_{\tau=\tau_0} \quad (2.13) \end{aligned}$$

In Eq. (2.10), the electromagnetic radiations of charged particles involves a tail term which gets contribution only from the spacetime curvature. Due to the presence of tail term, the EEP is invalid for the electromagnetic radiations of charged particles in curved spacetime. Nevertheless, as the leading order of the tail part is of $\mathcal{O}(\epsilon^0)$, if we focus on the photons with high enough frequency, the tail part can be dropped and only $F_{\mu\nu}^{(-2)}$ and $F_{\mu\nu}^{(-1)}$ terms survive. As a result, the EEP is valid for electromagnetic radiations of charged particles under the approximation of geometrical optics.

Moreover, the term $F_{\mu\nu}^{(-2)}$ corresponds to electromagnetic field generated by the Coulomb potential. And a nonvanishing $F_{\mu\nu}^{(-1)}$ would give a non-trivial electromagnetic radiations dependent on the 4-acceleration of charged particles $D_\tau Z^\alpha$. In other words, if the charged particles move along geodesic trajectories, this term would be vanishing, so we focus on the particles in non-geodesic motions in the following discussion.

When charged particles of mass m are only impacted by a magnetic field

$$D_\tau Z^\alpha = \frac{e}{m} F_\beta{}^\alpha Z^\beta, \quad (2.14)$$

the electromagnetic radiations are the so-called synchrotron radiations, which have an excellent property of polarizations encoding the information of the source and the magnetic field. Therefore, it is extremely interesting to have a careful study of the synchrotron radiation.

The electric vector can be extracted from the electric components in $F_{\mu\nu}^{(-1)}$ via a timelike tetrad

$$E^\mu \equiv \frac{1}{\epsilon} F^{(-1)\mu\nu} \xi_\nu, \quad (2.15)$$

where ξ_ν is the timelike component of a local Minkowski frame which can be chosen arbitrarily. The form of $F_{\mu\nu}^{(-1)}$ of a general electromagnetic wave can always be rewritten as

$$F_{\mu\nu}^{(-1)} \equiv k_\mu \mathcal{A}_\nu - k_\nu \mathcal{A}_\mu, \quad (2.16)$$

where \mathcal{A}_μ can be read from the expression (2.12)

$$\mathcal{A}_\mu = -4e \left[\bar{g}_{\mu\alpha} (k_\beta D_\tau Z^{[\beta} Z^{\alpha]}) (k_\eta Z^\eta)^{-3} \right]_{\tau=\tau_0}. \quad (2.17)$$

Taking into account of the conditions, $k \cdot k = 0$ and $k \cdot \mathcal{A} = 0$, we obtain the intensity of the synchrotron radiations

$$I_\xi = \epsilon^2 E^\mu E_\mu = (k_\rho \xi^\rho)^2 (\mathcal{A}_\sigma \mathcal{A}^\sigma), \quad (2.18)$$

observed by the observer ξ^μ . Considering the conserved quantity associated with the intensity along null geodesics, we can define the intensity observed by the observer with tetrad \hat{O} at infinity, $I_o = g^{-4} I_s$, with I_s being the intensity in the frame of the charged source $I_s = \nu_s^2 \mathcal{A}^2$, where $\nu_s = -k^\rho Z_\rho$ and $\nu_o = -k^\mu O_\mu$ are the frequencies of photons observed by the charged particles and the infinite observer, respectively, and $g = \nu_s / \nu_o$ is the redshift factor. After some calculations, we find the intensity observed at infinity

$$I_o = g^{-4} |k_\beta D_\tau Z^\beta Z^\alpha D_\tau Z^\alpha|_{\tau=\tau_0}^2. \quad (2.19)$$

Next, we move to the polarization vector of the synchrotron radiations. Considering the fact that the polarization vector $f^\mu \propto E^\mu$ should be normalized and transverse along the null geodesic, we have $f^\mu f_\mu = 1$, $f^\mu k_\mu = 0$. Note that a general polarization vector of the electromagnetic wave has four components, but with only one physical degree of freedom: apart from the two constraints, in fact, a gauge freedom exists. If we change ξ to ξ' , it is not hard to check that the variation $\delta f^\mu \equiv f'^\mu - f^\mu$ satisfies $\delta f^\mu \delta f_\mu = 0$, $\delta f^\mu k_\mu = 0$, which means that it is proportional to the 4-momentum of radiation, i.e., $\delta f^\mu \propto k^\mu$. In this sense, f'^μ is indistinguishable from f^μ : they differs from each other only by a gauge transformation proportional to k^μ . Moreover, from Eq. (2.16), we can see that $f^\mu \sim F^{(-1)\mu\nu} \xi_\nu = (\mathcal{A}_\nu \xi^\nu) k_\mu - (k_\nu \xi^\nu) \mathcal{A}_\mu$. The first term $(\mathcal{A}_\nu \xi^\nu) k_\mu \propto k_\mu$ can be gauged away, therefore without loss of generality, the polarization vector can be taken as

$$f_\mu = \frac{\mathcal{A}^\mu}{\sqrt{\mathcal{A}^2}} = N^{-1} \left[\bar{g}_{\mu\alpha} (k_\beta D_\tau Z^{[\beta} Z^{\alpha]}) \right]_{\tau=\tau_0}, \quad (2.20)$$

where we have normalized the vector appropriately.

The formulas (2.19) and (2.20) are the main results in our work. Obviously they may reduce to those in flat spacetime, in accord with the EEP. More importantly they can be applied to explore the polarized structure of synchrotron radiations in curved spacetime, without resorting coordinate transformations.

3 Polarization of synchrotron radiations around a Schwarzschild black hole

As an example, let us use Eq. (2.20) to exhibit polarization directions of synchrotron radiations in the Schwarzschild black hole spacetime. The metric takes in this form

$$ds^2 = -\left(1 - \frac{2M}{r}\right)dt^2 + \left(1 - \frac{2M}{r}\right)^{-1}dr^2 + r^2(d\theta^2 + \sin^2\theta d\phi^2), \quad (3.1)$$

where M is the mass of the black hole. For simplicity, we assume the black hole is immersed in a uniform magnetic field [25] with nonzero component of the gauge field ¹

$$A_\phi = \frac{1}{2}Br^2 \sin^2\theta, \quad (3.2)$$

where B is a constant standing for the strength of the uniform magnetic field. In particular, we want to emphasize that the model we consider here does not involve the backreaction of the magnetic field to the background spacetime, that is, the spacetime is still characterized by the Schwarzschild black hole metric.

3.1 The motion of source

In this work, the source of our interest are large numbers of electrons moving in the region near a Schwarzschild black hole. Since the Schwarzschild black hole is bathed in uniform magnetic fields, the equation of motion of electrons must include a Lorentz force term[27]. For such a equation, one cannot obtain a general analytical result. To simplify our discussions, we are going to constrain the charged particles to the equatorial plane vertical to the uniform magnetic field and let them move along circular orbits. Thus, the tangent vector of the world line of the source takes

$$Z^\alpha = (\dot{t}_s, \dot{r}_s, 0, \dot{\phi}_s), \quad (3.3)$$

¹The analysis of the polarized images employed by our method has been applied to a Melvin magnetic field in [26].

where, we have set $\theta_s = \pi/2$, $r_s = \text{const}$ with the subscript s signifying the source, and the $\dot{}$ means the derivative to the proper time τ . Considering the energy $E = -mZ_t$ and angular momentum $L = mZ_\phi + qA_\phi$ are conserved along the world line of the source, where m and q are the mass and the charge of the source, respectively, we can obtain

$$\dot{r}_s^2 = \mathcal{E}^2 - \left(1 - \frac{2M}{r_s}\right) + \left[1 + r_s^2 \left(\frac{\mathcal{L}}{r_s^2} - \mathcal{B}\right)^2\right] = 0, \quad (3.4)$$

from the normalization condition of 4-velocity, that is, $Z^\alpha Z_\alpha = -1$. Note that in Eq. (3.4), we reparameterize B, E, L as

$$\begin{aligned} \mathcal{B} &\equiv \frac{qB}{2m}, \\ \mathcal{E} &\equiv E/m = \dot{t}_s \left(1 - \frac{2M}{r_s}\right), \\ \mathcal{L} &\equiv L/m = \dot{\phi}_s r_s^2 + \mathcal{B} r_s^2, \end{aligned} \quad (3.5)$$

In our convention, \mathcal{B} is always set to be positive, thus, a positive \mathcal{L} corresponds to an antero-grade orbit and a negative one means retrograde, see a diagram in Fig. 2. It's obvious that a negative \mathcal{B} system is equivalent to a positive \mathcal{B} system via a reflection transformation. For circular orbits, one further has $\ddot{r}_s = 0$, which gives

$$r_s \left(\frac{\mathcal{L}}{r_s^2} - \mathcal{B}\right) \left[\frac{\mathcal{L}}{r_s^2} \left(1 - \frac{3M}{r_s}\right) + \mathcal{B} \left(1 - \frac{M}{r_s}\right)\right] - \frac{M}{r_s^2} = 0. \quad (3.6)$$

Note that, \mathcal{E} does not appear in Eq. (3.6), thus we can use this equation to identify the reparameterized angular momentum \mathcal{L} for given r_s and \mathcal{B} . Then, plunging \mathcal{L}, \mathcal{B} and r_s in Eq. (3.4), one can obtain the reparameterized energy \mathcal{E} . Then the 4-vector Z^α can be completely determined, that is, the initial conditions we need to know are the radius of the source orbit and the strength of the magnetic field around the black hole.

In addition, not all the timelike circular orbits are stable. For example, for a vacuum Schwarzschild black hole, timelike circular orbits inside $r = 6M$ are unstable, and the critical radius is known as the innermost stable circular orbit (ISCO). In the following, we would like to focus on the situation that the radial position of the source locates from $r_s = 6M$ to $r_s = 10M$.

3.2 Propagation of light and image of source

Beforehand, we have known the information of orbits of the source and the polarization vector of synchrotron radiations caused by the source. However, since our final task is to find out the information of the polarization of synchrotron radiations at the position of an observer

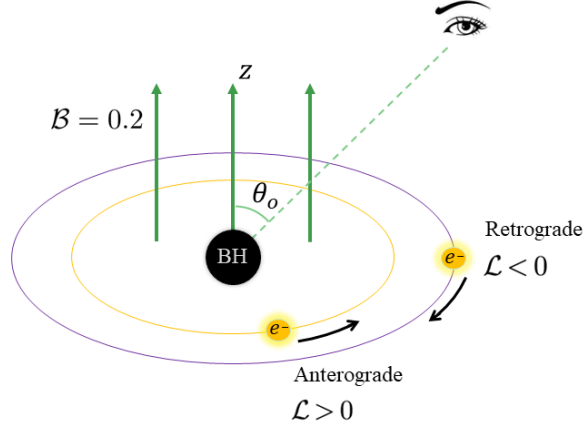


Figure 2: A diagram of retrograde ($\mathcal{L} < 0$) and anterograde ($\mathcal{L} > 0$) orbits of electrons. We set the direction of the magnetic field $\vec{\mathcal{B}}$ is along the positive axis of z . θ_o is the inclination of the observer.

which is generally placed at infinity, we have to figure out the propagation of electromagnetic waves from the source to the observer. For simplicity, we only consider high-frequency emissions, such that, we are allowed to use geometric optics approximation to deal with the propagation problem. That is to say, the emissions that breads away from the source go along null geodesics in the spacetime.

Null geodesics in Schwarzschild black hole spacetime have been studied very clearly[28]. Here we only introduce some basic physical quantities and useful formulas. In our convention, we use k^μ to denote the 4-momentum of photons. Note that there's spherical symmetry for Schwarzschild black hole and $\theta_s = \pi/2$, however, observers are not necessarily on the equatorial plane, thus k^θ cannot be set to be zero in general. Along null geodesics, there are three conserved quantites, that is, the energy ω and the angular-momentum l and Carter constant Q^2 , as

$$\omega = -k_t, \quad l = k_\phi, \quad Q^2 = k_\theta^2 + \frac{k_\phi^2}{\sin^2 \theta}. \quad (3.7)$$

Then, from $k^\mu k_\mu = 0$, one can find the results of k^μ ,

$$k^t/\omega = \left(1 - \frac{2M}{r}\right)^{-1}, \quad k^r/\omega = \pm \frac{\sqrt{R(r)}}{r^2}, \quad k^\theta/\omega = \pm \frac{\sqrt{\Theta(\theta)}}{r^2}, \quad k^\phi/\omega = \frac{\lambda}{r^2 \sin^2 \theta}, \quad (3.8)$$

where,

$$R(r) = r^4 - (r^2 - 2Mr)\rho^2, \quad (3.9)$$

$$\Theta(\theta) = \rho^2 - \frac{\lambda^2}{\sin^2 \theta}. \quad (3.10)$$

with impact parameters $\lambda \equiv l/\omega$ and $\rho^2 \equiv Q^2/\omega^2$. Next, consider an observer with the coordinate $(t_o, r_o, \theta_o, \phi_o)$. The position of photons reaching eyes of observers can be described by celestial coordinates which are usually chosen as

$$\begin{aligned}\alpha &= -\frac{\lambda}{\sin \theta_o}, \\ \beta &= \pm_o \sqrt{\Theta(\theta_o)},\end{aligned}\tag{3.11}$$

where $\pm_o = \text{sign}(k^\theta)$ denoting the sign of k^θ at the observer. Alternatively, for convenience, one can use polar coordinates (ρ, φ) instead of Cartesian coordinates (α, β) . The two coordinate frames are related by

$$\rho = \sqrt{\alpha^2 + \beta^2} = \frac{Q}{\omega}, \quad \tan \varphi = \frac{\beta}{\alpha}.\tag{3.12}$$

Then, consider null geodesics connecting the source $(t_s, r_s, \pi/2, \phi_s)$ to the source $(t_o, r_o, \theta_o, \phi_o)$. We integrate Eq. (3.8) and have

$$I_r = G_\theta, \quad \Delta\phi = \phi_o - \phi_s = \lambda G_\phi,\tag{3.13}$$

where,

$$I_r = \int_{r_s}^{r_o} \frac{dr}{\pm_r \sqrt{R(r)}}, \quad G_\theta = \int_{\pi/2}^{\theta_o} \frac{d\theta}{\pm_\theta \sqrt{\Theta(\theta)}}, \quad G_\phi = \int_{\pi/2}^{\theta_o} \frac{\csc^2 \theta d\theta}{\pm_\theta \sqrt{\Theta(\theta)}}\tag{3.14}$$

with the notation \int indicating that these integrals are path integrals along the photon trajectories. And the symbols $\pm_r = \text{sign}(k^r)$ and $\pm_\theta = \text{sign}(k^\theta)$ indicate the sign of k^r and k^θ , which switch at radial and angular turning points, respectively. Let \bar{m} be the number of the times that light rays cross the equatorial plane from the source to the observer. One can find

$$G_\theta = \frac{1}{\rho} \arccos\left(-\frac{\sin \varphi}{\sqrt{\sin^2 \varphi + \cot^2 \theta_o}}\right) + \frac{\bar{m}\pi}{\rho},\tag{3.15}$$

here and hereafter, we set $M = 1$ for simplicity and without loss of generality. In addition, different values of \bar{m} correspond to the $(\bar{m} + 1)$ th image on the observers' screen. In this work, we would like to focus on the primary and secondary image of the source. Now, from Eqs. (3.11-3.15), one can completely obtain the image of the source on the observer's screen given the spacetime coordinates of the source and observer.

3.3 Penrose-Walker constant

In this subsection, we move to study the transmission of polarization information along null geodesics connecting the source and observer. Note that, for spacetime of Petrov type-D

[16], there's a a conserved quantity along geodesics for a parallel-transported and transverse vector, dubbed as the Penrose-Walker(PW) constant which is typically written as

$$\kappa = 2r[(k^\mu \hat{l}_\mu)(f^\nu \hat{n}_\nu) - (k^\mu \hat{m}_\mu)(f^\nu \hat{m}_\nu)] \equiv \omega(\kappa_1 + i\kappa_2), \quad (3.16)$$

for Schwarzschild black hole spacetime, where, r is the radial coordinate introduced in the metric (3.1), k^μ is the 4-momentum of photons, f^μ is the polarization vector, $\kappa_{1,2}$ are rescaled real part and imaginary part of PW constant, and $\{\hat{l}^\mu, \hat{n}^\mu, \hat{m}^\mu, \hat{m}^{\mu*}\}$ are the Neumann-Penrose tetrads taking in the form

$$\begin{aligned} \hat{l} &= \frac{1}{\sqrt{2(1-\frac{2}{r})}} \left[\partial_t + \left(1 - \frac{2}{r}\right) \partial_r \right], \\ \hat{n} &= \frac{1}{\sqrt{2(1-\frac{2}{r})}} \left[\partial_t - \left(1 - \frac{2}{r}\right) \partial_r \right], \\ \hat{m} &= \frac{1}{\sqrt{2}r} \left[\partial_\theta + \frac{i}{\sin\theta} \partial_\phi \right], \\ \hat{m}^* &= \frac{1}{\sqrt{2}r} \left[\partial_\theta - \frac{i}{\sin\theta} \partial_\phi \right]. \end{aligned} \quad (3.17)$$

From Eq. (3.16), we can see that all the information of polarization is encoded in the PW constant at the source, thus considering the light rays connecting the source and the observer, we can decode the information of polarization at the observer. On the screen of observers, the polarization vector can be read from the PW constant as

$$\begin{aligned} \vec{\mathcal{E}} &= (\mathcal{E}_\alpha, \mathcal{E}_\beta), \\ &= \frac{1}{\rho^2} (\beta\kappa_2 + \alpha\kappa_1, \beta\kappa_1 - \alpha\kappa_2). \end{aligned} \quad (3.18)$$

Now, we have completed all the theoretical preparations and are ready to apply our model to some specific situations.

4 Specific examples

In this section, based on our model we would like to show some specific examples including considering sources in different orbits, background with different magnetic field strengths and et al. From Eqs. (2.14) and (2.20), we can see that the strength of the magnetic field B has no influence on the direction of the polarization vector, thus we fix $B = 0.2$ in the following.

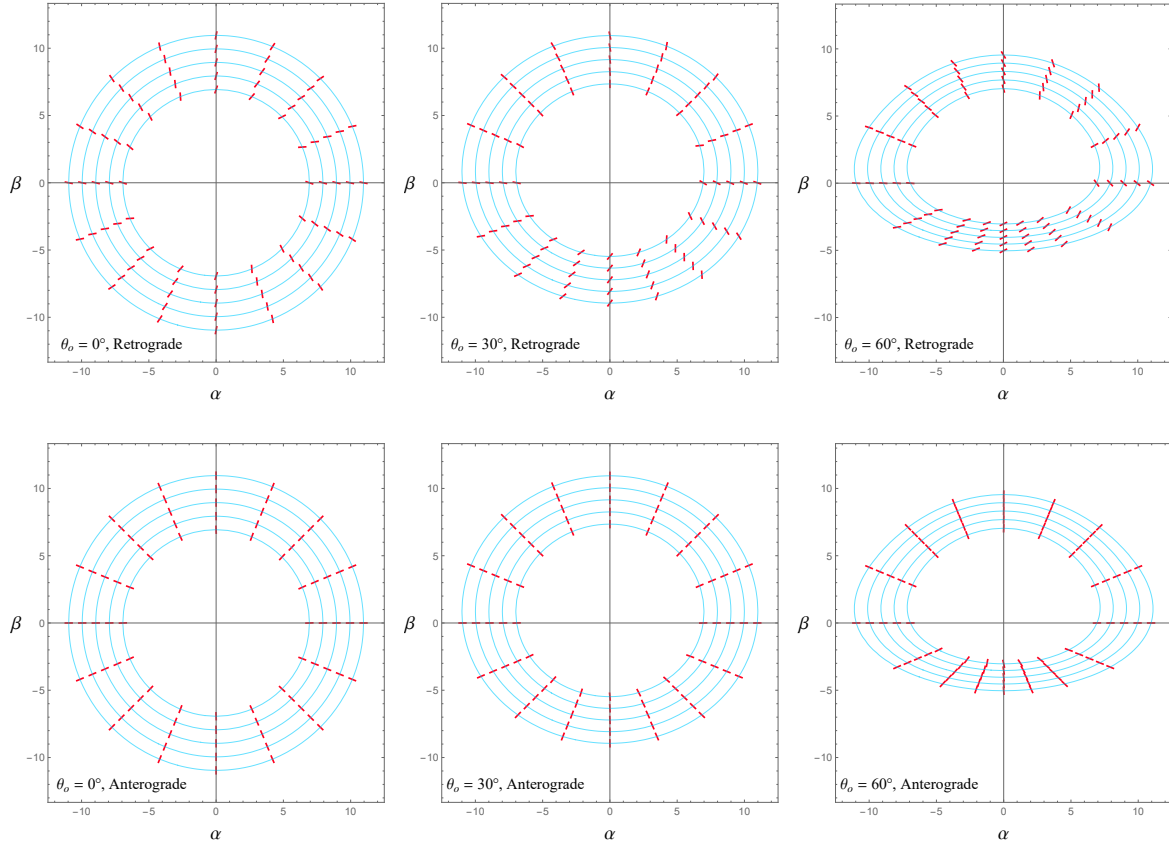


Figure 3: Primary images of sources and their polarization directions at $\mathcal{B} = 0.2$.

In Fig. 3, we show the the primary images of sources and their polarization directions for $\theta_o = 0, \pi/4, \pi/3$ at $\mathcal{B} = 0.2$. The upper panel shows the retrograde orbits and the lower one gives the results of anterograde orbits. The light blue cures are the images of source and the red lines stand for the polarization directions of some points. As well, the radii of the source orbits are $r_s = 6, 7, 8, 9, 10$ from the inside out.

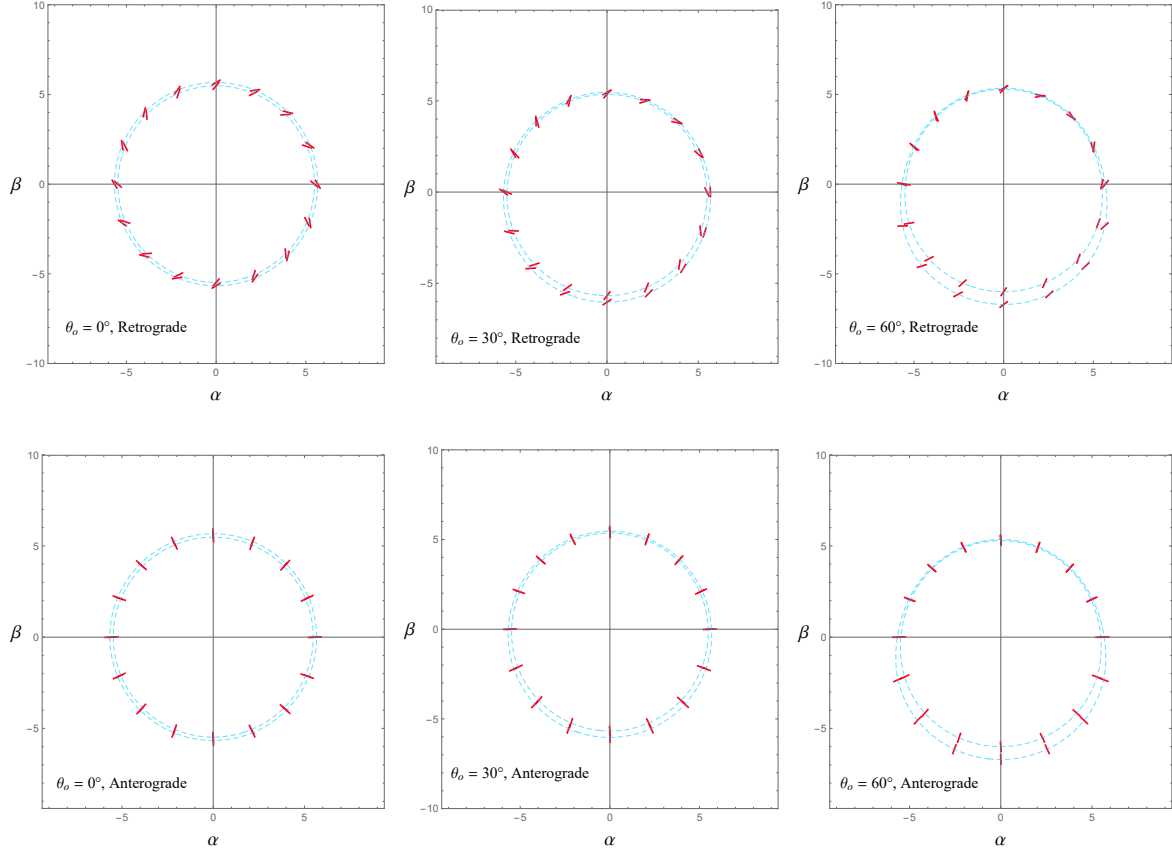


Figure 4: Secondary images of sources and polarization directions at $\mathcal{B} = 0.2$.

We also show the results of the secondary images of sources and polarization directions for $\theta_o = 0, \pi/4, \pi/3$ at $\mathcal{B} = 0.2$ in Fig. 4. Likewise, images of retrograde orbits are shown on the upper panel, and the lower shows the anterograde with the red lines and light blue curves indicating the polarization directions and orbits, respectively. However, we only show the orbits with $r_s = 6$ and $r_s = 10$ just to make the picture a little bit clearer, since there is some overlap between the secondary images of close orbits.

From Fig. 3 and Fig. 4, qualitatively we can see that for anterograde orbits the angles between polarization directions and the corresponding lines through the origin and the celestial coordinates are very small, that is to say the polarizations from anterograde orbits are more like pointing to the center of the screen of observers. While for retrograde orbits, the angles between polarization directions and the corresponding lines through the origin and the celestial coordinates become larger as the inclination of the observer θ_o increases in $[0, \pi/2]$.

In order to make the description of the polarization angle more intuitive, from Eqs. (3.12)

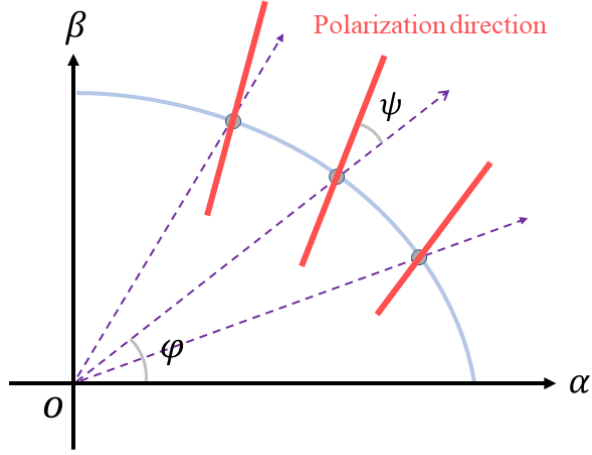


Figure 5: A diagram of a angle between the polarization vector and the radial vector at (ρ, φ) in the $\alpha - \beta$ plane.

and (3.18) we introduce a new angle defined as

$$\psi = -\arctan\left(\frac{\kappa_2}{\kappa_1}\right) + \frac{\text{sign}(\kappa_1) - 1}{2}\pi, \quad (4.1)$$

here, we specify that the angle ψ increases along the counterclockwise direction, for example, in Fig. 5, we have $\psi > 0$. Note that the term $\frac{\text{sign}(\kappa_1) - 1}{2}\pi$ is added to ensure the ψ function is continuous in $(-\pi, \pi)$, since arctan-function is usually defined in $[-\pi/2, \pi/2]$. Also, this term doesn't affect the polarization information since ψ and $\psi - \pi$ indicate the same polarized light in physics. Thus, we can see that after the vector at the angle of $\varphi \in [0, 2\pi]$ from the α -axis goes through a ψ rotation, it's going to be parallel to the polarization vector at the point (ρ, φ) on the $\alpha - \beta$ plane. Now, we are allowed to use ψ to quantitatively reflect the extent of which the polarization direction deviates from φ .

Considering the intensities of the secondary images are much lower than those of primary images, though we have not included the calculations of intensity in our model yet, we just show the results of ψ for primary images in Fig. 6.

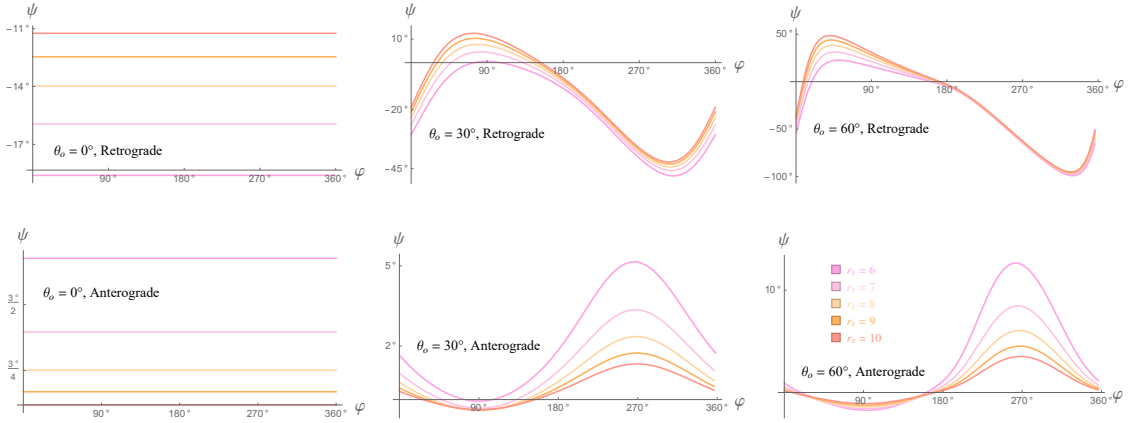


Figure 6: The variation of ψ with respect to φ for primary images.

From Fig. 6, we find that for anterograde and retrograde orbits, $|\psi|_{\max}$ becomes larger as $\theta_o \in [0, \pi/2]$ increases and the orbit radius $r_s \geq 6$ decreases. In particular, when $\theta_o = 0$, that is the observer is at the north or south pole, $\psi = 0$ is always true. However, compared with anterograde orbits, $|\psi|_{\max}$ of retrograde orbits at the same radius is much bigger, that is, the polarization structures are significantly different for anterograde and retrograde orbits. In addition, as a warm up, in this work we only apply our model a Schwarzschild black hole which has no spin, we have not been able to directly compare with the polarization images taken by EHT. But as far as the results are concerned, we can see that polarization structures of retrograde orbits in our models are more similar to those of the polarization image taken by EHT.

5 Conclusion

In this paper, we have given a universal covariant formula to describe the electromagnetic radiations of charged particles, which holds true for any curved spacetime. Although the radiation involves a tail term which invalidate the EEP, we showed that the EEP works well in the geometric optics approximation. Furthermore, we obtained compact covariant formulas characterizing the intensities and polarization directions of synchrotron radiations when charged particles are accelerated by a magnetic field in curved spacetime.

Then, we applied our model to a Schwarzschild black hole and built all specific formulas needed to determine the images and their polarization directions of sources travelling in circular orbits on the equatorial plane of a Schwarzschild black hole immersed in a vertical uniform magnetic fields in Sec. 3. We also showed the primary and secondary images and polarization directions in some specific situations considering various strengths of magnetic

fields, inclinations of observers for retrograde and anterograde orbits, as seen in Fig. 3 and Fig. 4. In particular, we introduced a new angle ψ to quantitatively describe the derivations of the polarizarion vector from the radial vector at (ρ, φ) on the celestial coordinate plane and an example of ψ was shown in Fig. 6. Some interesting behaviors of polarization directions of sources were also discussed.

We conclude this paper with some outlooks. First of all, the equation (2.19) can be straightforward applied to study the intensity of polarized radiations, which has not been included in our example. Obviously, to have a complete picture of synchrotron radiations, the intensity and distribution of radiations should be understood more thoroughly. Secondly, the environment outside a black hole is always messy. In a realistic rotational spacetime containing a black hole, complicated ingredients such as dark matter, jets and halo etc. should be taken into account. In order to have a good insight of the polarized images from EHT, one may have to appeal for an effective metric to describe a real spacetime. In this case, the effective metric could become very complicated and the so-called Penrose-Walker constant does not exist. Nevertheless, our discussion still works well in this situation. At last, the equation (2.20) may play a fundamental role in studying the radiations of accelerating charged particles in an arbitrary orbit. Based on our work, one could be allowed to catch a glimpse of different features for rdeflected, bound and plunging orbits from the polarization information in the images. For example the radiations from the particles in the plunging orbits may come to us without interacting with the plasma, as a result, they bring “clean” information on the spacetime geometry and the magnetic field configuration to us.

Acknowledgments

The work is in part supported by NSFC Grant No. 11735001, 11775022 and 11873044. MG is also supported by “the Fundamental Research Funds for the Central Universities” with Grant No. 2021NTST13.

References

- [1] B. S. Dewitt and R. W. Brehme, “Radiation damping in a gravitational field,” *Annals of Physics* **9** no. 2, (1960) 220–259.
- [2] **Event Horizon Telescope** Collaboration, K. Akiyama *et al.*, “First M87 Event Horizon Telescope Results. I. The Shadow of the Supermassive Black Hole,” *Astrophys. J. Lett.* **875** (2019) L1, [arXiv:1906.11238](https://arxiv.org/abs/1906.11238) [astro-ph.GA].

- [3] **Event Horizon Telescope** Collaboration, K. Akiyama *et al.*, “First M87 Event Horizon Telescope Results. VII. Polarization of the Ring,” *Astrophys. J. Lett.* **910** no. 1, (2021) L12, [arXiv:2105.01169 \[astro-ph.HE\]](#).
- [4] **Event Horizon Telescope** Collaboration, K. Akiyama *et al.*, “First M87 Event Horizon Telescope Results. VIII. Magnetic Field Structure near The Event Horizon,” *Astrophys. J. Lett.* **910** no. 1, (2021) L13, [arXiv:2105.01173 \[astro-ph.HE\]](#).
- [5] P. A. Connors, T. Piran, and R. F. Stark, “Polarization features of X-ray radiation emitted near black holes,” *Astrophys. J.* **235** (1080) 224–244.
- [6] B. C. Bromley, F. Melia, and S. Liu, “Polarimetric imaging of the massive black hole at the galactic center,” *Astrophys. J. Lett.* **555** (2001) L83, [arXiv:astro-ph/0106180](#).
- [7] A. E. Broderick and A. Loeb, “Imaging optically-thin hot spots near the black hole horizon of sgr a* at radio and near-infrared wavelengths,” *Mon. Not. Roy. Astron. Soc.* **367** (2006) 905–916, [arXiv:astro-ph/0509237](#).
- [8] L.-X. Li, R. Narayan, and J. E. McClintock, “Inferring the Inclination of a Black Hole Accretion Disk from Observations of its Polarized Continuum Radiation,” *Astrophys. J.* **691** (2009) 847–865, [arXiv:0809.0866 \[astro-ph\]](#).
- [9] J. D. Schnittman and J. H. Krolik, “X-ray Polarization from Accreting Black Holes: II. The Thermal State,” *Astrophys. J.* **701** (2009) 1175–1187, [arXiv:0902.3982 \[astro-ph.HE\]](#).
- [10] R. V. Shcherbakov, R. F. Penna, and J. C. McKinney, “Sagittarius A* Accretion Flow and Black Hole Parameters from General Relativistic Dynamical and Polarized Radiative Modeling,” *Astrophys. J.* **755** (2012) 133, [arXiv:1007.4832 \[astro-ph.HE\]](#).
- [11] R. Gold, J. C. McKinney, M. D. Johnson, and S. S. Doeleman, “Probing the Magnetic Field Structure in Sgr A on Black Hole Horizon Scales with Polarized Radiative Transfer Simulations,” *Astrophys. J.* **837** no. 2, (2017) 180, [arXiv:1601.05550 \[astro-ph.HE\]](#).
- [12] M. Moscibrodzka, J. Dexter, J. Davelaar, and H. Falcke, “Faraday rotation in GRMHD simulations of the jet launching zone of M87,” *Mon. Not. Roy. Astron. Soc.* **468** no. 2, (2017) 2214–2221, [arXiv:1703.02390 \[astro-ph.HE\]](#).
- [13] A. Jiménez-Rosales and J. Dexter, “The impact of Faraday effects on polarized black hole images of Sagittarius A*,” *Mon. Not. Roy. Astron. Soc.* **478** no. 2, (2018) 1875–1883, [arXiv:1805.02652 \[astro-ph.HE\]](#).

- [14] F. Marin, M. Dovciak, F. Muleri, F. F. Kislat, and H. S. Krawczynski, “Predicting the X-ray polarization of type-2 Seyfert galaxies,” *Mon. Not. Roy. Astron. Soc.* **473** no. 1, (2018) 1286–1316, [arXiv:1709.03304 \[astro-ph.HE\]](#).
- [15] D. C. M. Palumbo, G. N. Wong, and B. S. Prather, “Discriminating Accretion States via Rotational Symmetry in Simulated Polarimetric Images of M87,” *Astrophys. J.* **894** no. 2, (2020) 156, [arXiv:2004.01751 \[astro-ph.HE\]](#).
- [16] A. Lupsasca, D. Kapec, Y. Shi, D. E. A. Gates, and A. Strominger, “Polarization whorls from M87* at the event horizon telescope,” *Proc. Roy. Soc. Lond. A* **476** no. 2237, (2020) 20190618, [arXiv:1809.09092 \[hep-th\]](#).
- [17] **Event Horizon Telescope** Collaboration, R. Narayan *et al.*, “The Polarized Image of a Synchrotron-emitting Ring of Gas Orbiting a Black Hole,” *Astrophys. J.* **912** no. 1, (2021) 35, [arXiv:2105.01804 \[astro-ph.HE\]](#).
- [18] A. Ricarte, R. Qiu, and R. Narayan, “Black hole magnetic fields and their imprint on circular polarization images,” *Mon. Not. Roy. Astron. Soc.* **505** no. 1, (2021) 523–539, [arXiv:2104.11301 \[astro-ph.HE\]](#).
- [19] Z. Gelles, E. Himwich, D. C. M. Palumbo, and M. D. Johnson, “Polarized image of equatorial emission in the Kerr geometry,” *Phys. Rev. D* **104** no. 4, (2021) 044060, [arXiv:2105.09440 \[gr-qc\]](#).
- [20] Z. Zhang, S. Chen, X. Qin, and J. Jing, “Polarized image of a Schwarzschild black hole with a thin accretion disk as photon couples to Weyl tensor,” *Eur. Phys. J. C* **81** no. 11, (2021) 991, [arXiv:2106.07981 \[gr-qc\]](#).
- [21] V. Karas, M. Zajacek, D. Kunneriath, and M. Dovciak, “Electromagnetic signatures of strong-field gravity from accreting black-holes,” *Adv. Space Res.* **69** (2022) 448–466, [arXiv:2110.11136 \[astro-ph.HE\]](#).
- [22] X. Qin, S. Chen, and J. Jing, “Polarized image of an equatorial emitting ring around a 4D Gauss-Bonnet black hole,” [arXiv:2111.10138 \[gr-qc\]](#).
- [23] J. D. Jackson, “Classical Electrodynamics,”.
- [24] J. Hobbs, “A Vielbein Formalism of Radiation Damping,” *Annals of Physics* **47** (1968) 141–165.
- [25] R. M. Wald, “Black hole in a uniform magnetic field,” *Phys. Rev. D* **10** (1974) 1680–1685.

- [26] H. Zhu and M. Guo, “Polarized image of synchrotron radiations of hotspots in Schwarzschild-Melvin black hole spacetime,” [arXiv:2205.04777 \[gr-qc\]](#).
- [27] V. P. Frolov and A. A. Shoom, “Motion of charged particles near weakly magnetized Schwarzschild black hole,” *Phys. Rev. D* **82** (2010) 084034, [arXiv:1008.2985 \[gr-qc\]](#).
- [28] S. E. Gralla and A. Lupsasca, “Lensing by Kerr Black Holes,” *Phys. Rev. D* **101** no. 4, (2020) 044031, [arXiv:1910.12873 \[gr-qc\]](#).